Satellite remote sensing of particulate matter and air quality assessment over global cities

Pawan Gupta[a], Sundar A. Christopher[a,*], Jun Wang[b],
Robert Gehrig[c], Yc Lee[d], Naresh Kumar[e,f]

[a]*Department of Atmospheric Sciences, The University of Alabama in Huntsville, Huntsville, AL, USA*
[b]*NOAA/UCAR Postdoctoral Fellow, Department of Earth and Planetary Science, Harvard University, MA, USA*
[c]*EMPA, Laboratory for Air Pollution, Dubendorf, Switzerland*
[d]*Green Council, New World Tower 1, Hong Kong*
[e]*University of Iowa, Iowa City, IA, USA*
[f]*Brown University, Providence, RI, USA*

Abstract

Using 1 year of aerosol optical thickness (AOT) retrievals from the MODerate resolution Imaging Spectro-radiometer (MODIS) on board NASA's Terra and Aqua satellite along with ground measurements of $PM_{2.5}$ mass concentration, we assess particulate matter air quality over different locations across the global urban areas spread over 26 locations in Sydney, Delhi, Hong Kong, New York City and Switzerland. An empirical relationship between AOT and $PM_{2.5}$ mass is obtained and results show that there is an excellent correlation between the bin-averaged daily mean satellite and ground-based values with a linear correlation coefficient of 0.96. Using meteorological and other ancillary datasets, we assess the effects of wind speed, cloud cover, and mixing height (MH) on particulate matter (PM) air quality and conclude that these data are necessary to further apply satellite data for air quality research. Our study clearly demonstrates that satellite-derived AOT is a good surrogate for monitoring PM air quality over the earth. However, our analysis shows that the $PM_{2.5}$–AOT relationship strongly depends on aerosol concentrations, ambient relative humidity (RH), fractional cloud cover and height of the mixing layer. Highest correlation between MODIS AOT and $PM_{2.5}$ mass is found under clear sky conditions with less than 40–50% RH and when atmospheric MH ranges from 100 to 200 m. Future remote sensing sensors such as Cloud-Aerosol Lidar and Infrared Pathfinder Satellite Observations (CALIPSO) that have the capability to provide vertical distribution of aerosols will further enhance our ability to monitor and forecast air pollution. This study is among the first to examine the relationship between satellite and ground measurements over several *global locations*.
© 2006 Elsevier Ltd. All rights reserved.

Keywords: Aerosols; Satellite remote sensing; Air quality; Mega cities

1. Introduction

Almost half of the present world's population now lives in urban areas and their numbers will increase to four billion by the end of this decade

*Corresponding author.
E-mail address:* sundar@nsstc.uah.edu (S.A. Christopher).

(World urbanization prospects, 2003). Particulate matter (PM) (or aerosols) is one of the major pollutants that affect air quality in urban and even rural areas of the world. PM is a complex mixture of solid and liquid particles that vary in size and composition, and remain suspended in the air. PM with aerodynamic diameters less than $2.5 \mu m$ ($PM_{2.5}$) can cause respiratory and lung diseases and even premature death (Krewski et al., 2000). Atmospheric aerosols include both natural (wind-blown dust, sea salt from the oceans, and volcanic eruptions) and anthropogenic sources (aerosols from biomass burning, combustion from automobiles and emission from power plants) also play an important role in climate processes (e.g. Kaufman et al., 2002). Monitoring particulate pollution has attracted new interest with recent scientific evidence of the ill-health effects of small particles (e.g. Pope, 2000). For example, tens of thousands of premature deaths in Europe have been associated with increased exposure to PM (Leeuwen and Rolaf, 2002). The Tata Energy Research Institute (TERI) in India estimated 18,600 premature deaths per year associated with poor air quality in the Delhi region (TERI, 2001).

To understand the effects of PM on the earth's climate system and human health, it is necessary to routinely monitor $PM_{2.5}$ on a global basis. This task is challenging because these sub-micron aerosols are highly variable in space and time. Typically, using ground-based instruments, $PM_{2.5}$ mass concentration of ambient particles is widely measured in both urban and rural areas of Europe, United States, Australia, and Asia. However these ground-based observations represent point measurements and do not have the necessary coverage to map the regional to global distribution of aerosols. On the other hand, recent satellite data from the MODIS (Chu et al., 2003; Wang and Christopher., 2003) or Multi angle Imaging Spectro-Radiometer (MISR) (Liu et al., 2004) have tremendous potential for mapping global distribution of aerosols and their properties and for deriving indirect estimates of PM, particularly $PM_{2.5}$. Since ground measurements of $PM_{2.5}$ are sparse in many regions of the world satellite data could serve as surrogates for monitoring particulate matter air quality.

The potential for monitoring PM air quality using satellite data from space-based sensors from regional to global scales has been recently demonstrated using aerosol optical thickness (AOT) data (e.g. Wang and Christopher, 2003; Chu et al., 2003;

Engel-Cox, et al., 2004). The AOT is the integral of atmospheric extinction from the surface to the top of the atmosphere (TOA). This columnar retrieved parameter is dependent on aerosol mass concentration, mass extinction efficiency, hygroscopic growth factor, and effective aerosol scale height. Most studies to date have been restricted to the Continental United States and the current study fills the gap by presenting quantitative relationships between satellite-based AOT and $PM_{2.5}$ mass over several locations around the globe.

Although the satellite-based retrieval of air quality is promising, it poses several challenges. There are many factors that can affect the relationship between AOT and $PM_{2.5}$. For example, the satellite-derived quantities provide columnar information for ambient conditions whereas the $PM_{2.5}$ measurements are representative of near-surface dry mass concentrations. The satellite footprints represent large spatial areas and are subject to cloud contamination (Zhang et al., 2005). Other issues including variations in aerosol type and hygroscopicity must be adequately understood before using satellite data for air quality assessment. In the present study MODIS-derived AOT at $0.55 \mu m$ from two satellites, Terra and Aqua, is compared with the several ground-based $PM_{2.5}$ mass concentrations ($\mu g m^{-3}$) spread over India, Australia, Hong Kong, Switzerland, and United States. A sensitivity study is also performed over selected locations to quantify the effects of atmospheric mixing height (MH), relative humidity (RH) and cloud cover on the relationship between MODIS AOT and $PM_{2.5}$ mass concentrations.

2. Data and methods

The MODIS sensors on board Terra and Aqua satellites have 36 spectral channels providing information about atmospheric, land, and oceanic conditions. The MODIS provides observations in moderate spatial (from $250 m$–$1 km$) and temporal (1–2 day) resolutions in different spectral regions of the electromagnetic spectrum. The AOT algorithm uses observed radiances in seven wavelengths (0.47–$2.13 \mu m$) over ocean and two wavelengths (0.47, and $0.67 \mu m$) over land and pre-computed look up tables to retrieve AOT (Remer et al., 2005). Over land, the reported accuracy of MODIS AOT is $\pm 0.05 \pm 0.15 \tau$ when compared with several ground-based AERONET measurements, except in situations with (a) possible cloud contamination, (b) over

surfaces with sub pixel water such as coastal areas and marshes, and (c) over surfaces with sub pixel snow or ice cover. On a global basis, about 68% AOT retrievals fall within expected errors (Remer et al., 2005). The level 2 AOT data (at $0.55\,\mu m$) with a spatial resolution of $10 \times 10\,km^2$ (MOD04) retrieved from MODIS and $PM_{2.5}$ mass concentration ($\mu g\,m^{-3}$) from 26 air quality monitoring stations (Table 1) is used. This is the best available resolution at this time and therefore does not allow for studies requiring finer spatial scales. The MODIS level 2 daily AOT products from Terra (MOD04 V003) for January–December 2002 and from Aqua (MYD04 V003) for July–December 2002 is obtained for all study regions. Similar AOT data for Delhi is obtained for the period of July–November 2003. Apart from level 2, MODIS level 3 monthly mean AOT data in $1° \times 1°$ grid resolution from March 2000 to February 2002 is used to discuss the spatial distribution of AOT over the globe.

In the United States, Australia and Hong Kong, the $PM_{2.5}$ is measured using a Tapered-Element Oscillating Microbalance (TEOM) instrument with an accuracy of $\pm 1.5\,\mu g\,m^{-3}$ for hourly averages. In Switzerland, High Volume Samplers (HSV) Digital DA 80 instrument with an uncertainty of $\pm 10\%$ is used. In Delhi, PM data were collected using portable Aerocet 531 (Met One Instrument Inc.) at 113 sites from 23 July to 04 November 2003. Since these 113 sites were spread over an area of $40\,km^2$, these data were grouped into six regions (Fig. 1). The $PM_{2.5}$ data for USA sites are obtained from the EPA-AirNow database. The NOAA HYbrid Single-Particle Lagrangian Integrated Trajectory (HYSPLIT) model is used to calculate air mass back trajectories for 24-h interval with a total run time of 10 days (Draxler, 2003).

The MODIS AOT and $PM_{2.5}$ mass were collocated in space and time for inter-comparative and quantitative analysis. To match the datasets in time, all the observations within one hour were averaged.

Table 1
Detail information about all $PM_{2.5}$ stations

No.	Country	Station name	Latitude	Longitude	AOT$\pm$STD	$PM_{2.5}\pm$STD	N^*	R^*	Station type
1	India	Delhi 1 (NE)	28.684N	77.291E	0.77 ± 0.41	36.3 ± 15.9	6	0.24	Mix of RS and UP
2	India	Delhi 2 (N)	28.684N	77.187E	0.80 ± 0.61	38.0 ± 24.2	25	0.66	Mix of RS and UP
3	India	Delhi 3 (NW)	28.684N	77.084E	0.90 ± 0.95	51.0 ± 33.5	14	0.85	Mix of RS and UP
4	India	Delhi 4 (SE)	28.550N	77.291E	0.62 ± 0.26	52.3 ± 37.4	9	0.72	Mix of RS and UP
5	India	Delhi 5 (S)	28.550N	77.187E	0.67 ± 0.31	40.4 ± 30.0	23	0.41	Mix of RS and UP
6	India	Delhi 6 (SW)	28.550N	77.084E	0.74 ± 0.35	57.4 ± 75.6	8	0.65	Mix of RS and UP
7	Australia	Earlwood	33.917S	151.134E	0.25 ± 0.15	12.8 ± 6.10	308	0.32	PR
8	Australia	Lidcombe	33.886S	151.042E	0.30 ± 0.12	15.0 ± 5.80	116	0.48	Mix of RA and CA
9	Australia	Richmond	33.618S	150.746E	0.10 ± 0.08	16.2 ± 7.50	233	0.11	Mix of RA, RuA
10	Australia	Westmead	33.800S	150.996E	0.12 ± 0.10	11.0 ± 7.00	247	0.31	Golf course, RA area
11	Australia	Woolooware	34.044S	151.141E	0.20 ± 0.13	13.8 ± 6.20	168	0.32	Mix of RS and RA
12	Hong Kong	Causeway Bay	22.283N	114.183E	0.41 ± 0.20	60.0 ± 17.0	147	0.51	Mix of RS, UP, CA
13	Hong Kong	Central	22.283N	114.150E	0.42 ± 0.21	53.5 ± 21.1	142	0.54	Mix of RS, UP, CA
14	Hong Kong	Tung Chung	22.283N	113.950E	0.41 ± 0.21	40.2 ± 20.5	154	0.34	New Town, RA
15	Hong Kong	Tap Mun	22.467N	114.350E	0.42 ± 0.22	34.5 ± 17.4	162	0.49	RuA
16	Hong Kong	Tsuen Wan	22.367N	114.100E	0.41 ± 0.25	40.0 ± 18.2	132	0.38	Mix of RA, UP,CA
17	Switzerland	Basel	47.567N	7.600E	0.23 ± 0.14	19.6 ± 8.50	211	0.21	Mix of PA, UP
18	Switzerland	Bern	46.917N	7.467E	0.18 ± 0.11	21.4 ± 6.70	223	0.35	Mix of RS, UP
19	Switzerland	Chaumont	47.017N	6.950E	0.20 ± 0.14	15.0 ± 8.10	210	0.29	RuA, high altitude
20	Switzerland	Lugano	46.000N	8.967E	0.25 ± 0.19	22.5 ± 13.5	240	0.40	Mix of PA, UP
21	Switzerland	Payerne	46.490N	6.933E	0.16 ± 0.10	15.6 ± 7.50	200	0.45	RuA, close to town
22	USA	NewYork1	40.919N	73.994W	0.34 ± 0.22	15.2 ± 12.0	268	0.75	Mix of CA, UP
23	USA	NewYork2	40.671N	73.963W	0.47 ± 0.26	13.6 ± 11.9	214	0.48	Mix of CA, UP
24	USA	NewYork3	40.752N	73.977W	0.46 ± 0.25	16.0 ± 13.5	232	0.55	Mix of CA, UP
25	USA	NewYork4	40.737N	73.850W	0.45 ± 0.25	14.5 ± 12.0	247	0.60	Mix of CA, UP
26	USA	NewYork5	40.583N	74.163W	0.38 ± 0.22	13.7 ± 13.5	234	0.66	Mix of CA, UP

RD: road side, CA: city area, CA: commercial area, RA: residential, UP: urban populated, PR: park residential, RuA: rural area, STD: standard deviation, N: number of data points, R: liner correlation coefficient. Here AOT and $PM_{2.5}$ values are hourly averaged values during MODIS overpass time.
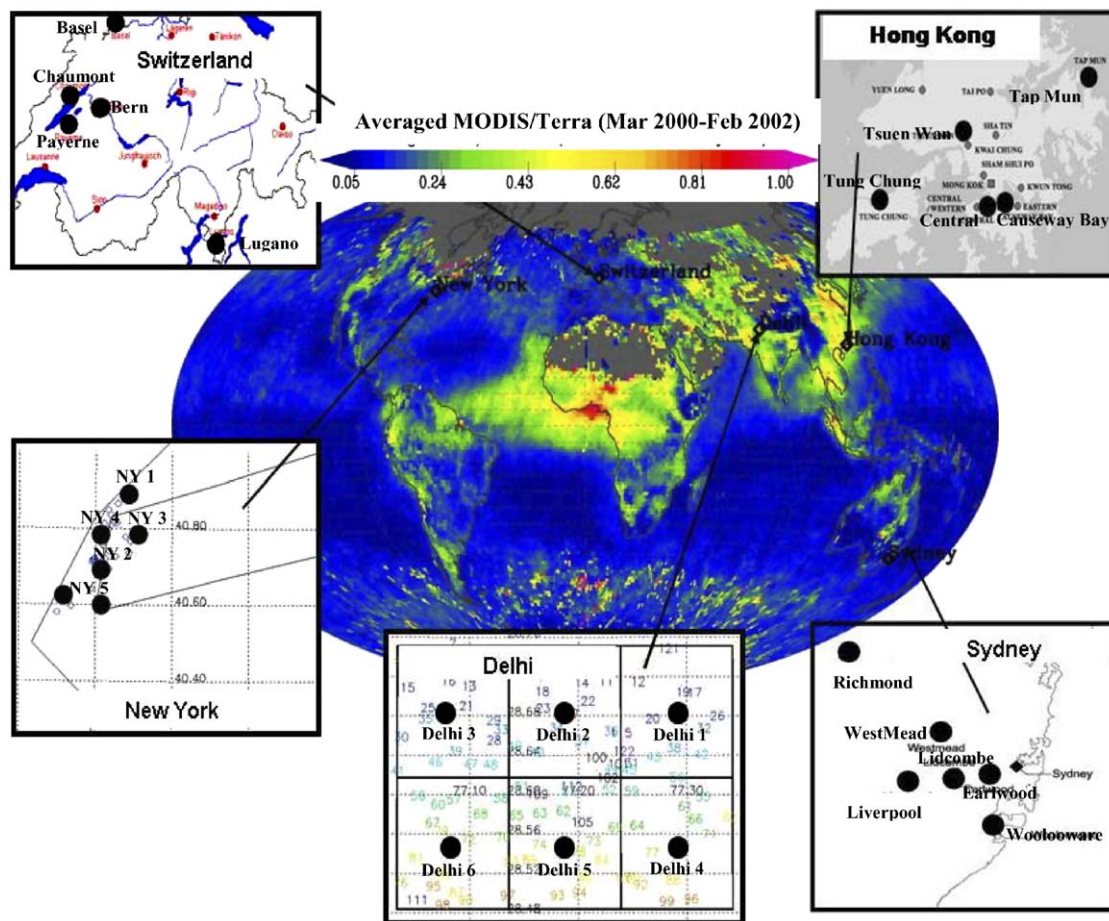
Fig. 1. Global distribution of the MODIS aerosol optical thickness during March 2000–February 2002. Insets show details of locations where PM$_{2.5}$ and MODIS AOT were compared.

Geographical collocation of MODIS pixels with PM$_{2.5}$ stations is performed by calculating the distance between the MODIS pixel and PM$_{2.5}$ station using latitude and longitude information. All the MODIS pixels within a distance of 0.2° (about 20–25 km) are averaged over PM$_{2.5}$ stations. One year (2002) of coincident data of PM$_{2.5}$ mass, MODIS AOT, MODIS cloud fraction, wind speed and RH obtained over five stations in Texas, United States of America (Table 2) are used to perform sensitivity studies to assess uncertainties.

3. Results and discussion

Our analysis begins with the description of worldwide distribution of AOT. Fig. 1 presents the global distribution of AOT averaged from March 2000 to February 2002. Dark gray regions denote missing data or no retrievals. The high AOT

values observed over Africa are due to dust outflow from Saharan regions. High frequency of dust events in dry seasons is mainly responsible for the poor air quality over Africa during spring and summer compared to other seasons. Apart from the dust outbreak in the dry season, urban and industrial pollution during summer time in eastern China, northern India, eastern United States, and parts of Europe are also partially responsible for the high concentration of aerosols observed in these regions (Chu et al., 2003). Dry season biomass burning in the southern hemisphere is also visible over South America and Africa.

Fig. 2(a–e) shows the monthly mean PM$_{2.5}$ mass concentration (solid dots), and MODIS AOT (square) for several locations. The thick solid and long dash lines are interpolated lines of PM$_{2.5}$ and AOT, respectively. Also shown are the 24-h mean values of PM$_{2.5}$ mass (small dotted line) for the
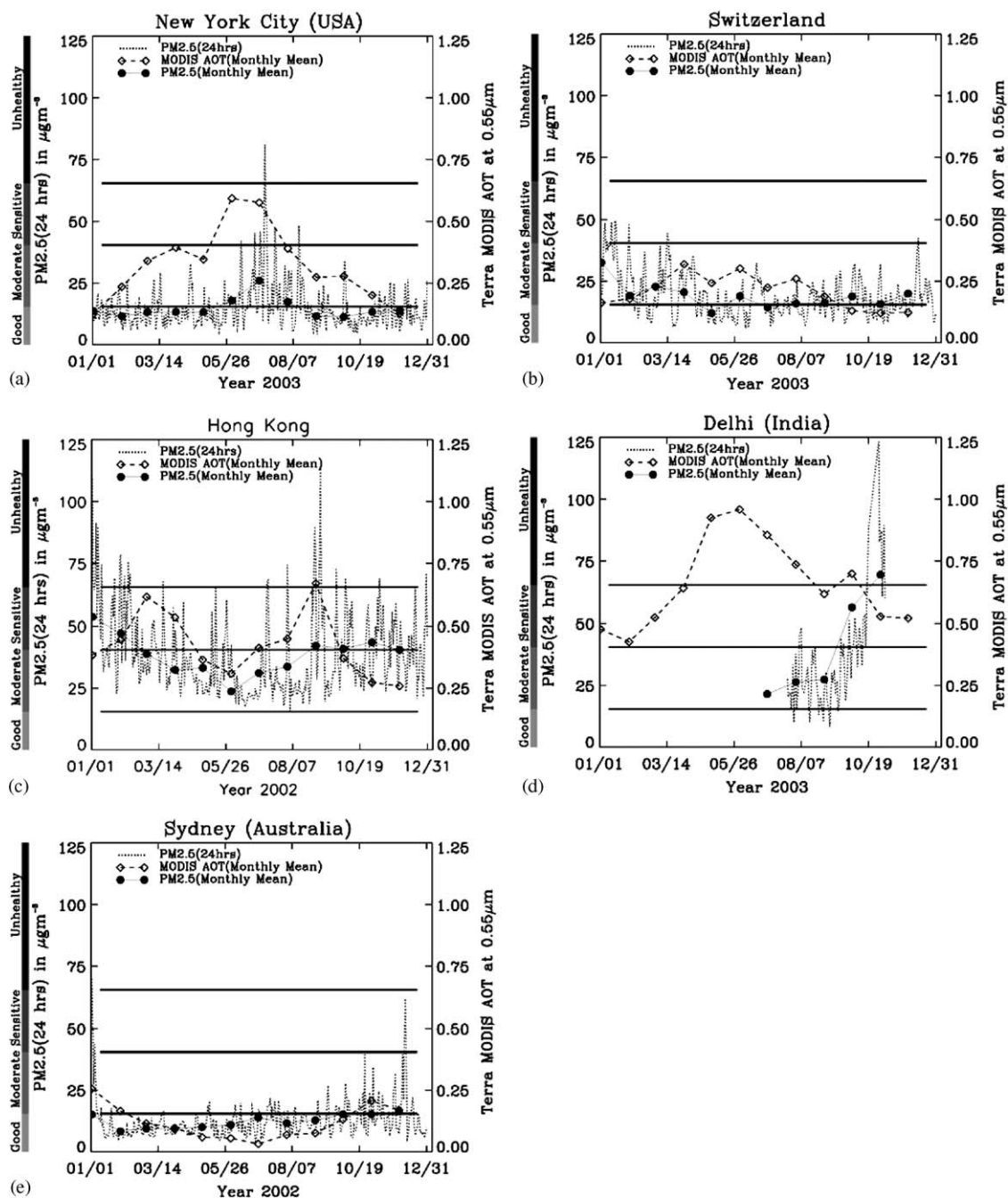
Fig. 2. Variations in $PM_{2.5}$ mass concentration ($\mu g\,m^{-3}$) and MODIS aerosol optical depth at 0.55 μm over all five study regions during 2002 except data from Delhi is for year 2003. (a) New York City (USA), (b) Switzerland (c) Hong Kong (d) Delhi (India) and (e) Sydney (Australia). The gray color bar shows the air quality index based on $PM_{2.5}$ mass concentration according to US EPA standards.

entire study period. Fig. 2 also includes the air quality categories represented by horizontal solid lines along with gray color-coded bar representing air quality condition in each region based on $PM_{2.5}$ mass loading. These air quality categories are

categorized according to the United States EPA Air Quality Index and we use this as a reference while recognizing that air quality standards in other countries could be different. The air quality category is called good if daily mean $PM_{2.5}$ mass

concentrations between 0–15.4 $\mu g\,m^{-3}$, moderate if between 15.4 and 40.4 $\mu g\,m^{-3}$, unhealthy for sensitive groups such as children and older adults if between 40.5 and 65.4 $\mu g\,m^{-3}$, unhealthy if between 65.5 and 150.4 $\mu g\,m^{-3}$ and very unhealthy if between 150.5 and 250.4 $\mu g\,m^{-3}$ (United States Environmental Protection Agency (USEPA), 2003).

It is important to note that $PM_{2.5}$ and MODIS AOT represent two different atmospheric loadings of pollutants. The $PM_{2.5}$ is the dry mass of aerosols measured at ground level and represents the particle mass concentration with aerodynamic diameter less than 2.5 μm. A recent study by Zheng et al. (2005) in Beijing, China, showed that dust contributed 36% to $PM_{2.5}$ mass. In regions with relatively low dust concentrations such as Switzerland, the mineral dust contributes 5–10% to the total $PM_{2.5}$ mass (Hueglin et al., 2005). On the other hand, the MODIS AOT represents total columnar loading of all aerosol particles from the surface to the TOA averaged over a large spatial area ($10 \times 10\,km^2$). Although differences are to be expected in these comparisons, it is important to develop air quality indices based on satellite data especially for regions that have very few ground observations. The relationship between $PM_{2.5}$ mass measured at ground and columnar AOT could also be different due to variations in source regions and aerosol transportation at different heights. The contribution of boundary layer aerosols could be different in column measurements (Franke et al., 2003) and layers in different heights can have different chemical and physical composition (Slater and Dibb, 2004). However, vertical profiles of aerosol obtained from observations show maximum concentrations near-ground and up to the boundary layer (Kaufman et al., 2003). The mean $PM_{2.5}$ values are less (0–25 $\mu g\,m^{-3}$) over clean environments like Sydney and Switzerland and greater (0–60 $\mu g\,m^{-3}$) over relatively highly polluted regions like Hong Kong, New York City, and Delhi. There are occasions when $PM_{2.5}$ mass values reached more than 100 $\mu g\,m^{-3}$ over Delhi, and Hong Kong, which could be attributed to possible local aerosol events reported in surrounding areas.

Ten day back trajectory analysis indicates that air masses originating in the Indian Ocean travel through arid and semi arid dust source regions in Oman, Pakistan, and India and then reach Delhi. Air masses reaching Sydney can originate over the Indian Ocean during Southern Hemisphere summer whereas during winter months they originate from inland regions of Australia. Pollution carried by these air masses is trapped in the Sydney basin due to its lower elevation relative to its surrounding areas. Smoke aerosols from Indonesian fires during June–August can be transported to Hong Kong. During the spring, air masses originating in Northern China may carry dust particles during heavy dust storms in the arid and semi arid regions. Switzerland experiences anthropogenic aerosols coming from North-East America, dust from Sahara regions, and pollution from Canada (mostly smoke from fires); which even reaches the Western United States and sometimes extends to New York (Hoff et al., 2005).

Seasonal variation in AOT over New York City corresponds well with the $PM_{2.5}$ trends (Fig. 2(a)); peak concentration of $PM_{2.5}$ were observed in July with a value of 28 $\mu g\,m^{-3}$ (monthly mean), whereas AOT values were highest for the month of June with a value of 0.6, and the difference between June and July was relatively small (0.02). The air quality in the city continues to remain under the 'good' category throughout the year except during summer months (June–August) when it reaches the 'moderate' category in agreement with the study by Schwab et al. (2004). High values of $PM_{2.5}$ and AOT during July are associated with the transport of smoke from Canada (Schwab et al., 2004). Fig. 2(b) shows the monthly mean AOT and $PM_{2.5}$ mass over Switzerland. Maximum $PM_{2.5}$ values during winter months and minimum during summer months are consistent with previous research studies conducted in this area (Hazenkamp-von Arx et al., 2003, 2004). A peak AOT value of 0.3 was observed in the month of April whereas $PM_{2.5}$ peak (35 $\mu g\,m^{-3}$) was found in January. $PM_{2.5}$ values were as high as 81.3 $\mu g\,m^{-3}$ with low values of 3.3 $\mu g\,m^{-3}$ during the study period. The monthly mean air quality is in the moderate category throughout the year except in May and July when the air quality is 'good'. The AOT and $PM_{2.5}$ values show similar monthly variations from April through September. Switzerland has many sources of air pollution like dust transported from Sahara deserts but the major part of $PM_{2.5}$ comes from vehicular emission as reported by roadside monitoring stations (Gehrig and Buchmann, 2003). The detailed correlation analysis over New York City shows a range of correlation coefficients 0.48–0.75 over different stations with overall values of 0.60. The seasonal analysis shows high linear correlations (0.76) during the winter season

compared to low values (0.45) in the summer months. This could be due to the fact that, this sulfate dominant region scatters more light in the summer months due to high RH and in turn produces high AOT. The same aerosol mass then produces less scattering in winter months compared to summer and hence AOT more accurately represents $PM_{2.5}$ mass. Apart from sulfate, the other aerosol types in this region are ammonium compounds, nitrates, and trace amount of metal in the form of dust (Schwab et al., 2004).

During spring and summer months, the air quality in Hong Kong remains in the moderate category with monthly mean $PM_{2.5}$ values ranging from 25 to $40 \mu g\,m^{-3}$ (Fig. 2(c)). The AOT over Hong Kong shows a bimodal distribution during the year whereas $PM_{2.5}$ shows a unimodal distribution. Research by Duce et al. (1980) demonstrated that the dust transported from the Gobi and Taklamakan deserts in China increases AOT concentration in Hong Kong during spring, and dust transport depends on the prevalence of the northeast monsoon (Lee and Hills, 2003). The maximum hourly $PM_{2.5}$ mass is as high as $133.5 \mu g\,m^{-3}$ and the corresponding AOT value is 1.1 during the winter season. For urban areas like Tsuen Wan, pollution sources are partly local and contributions come from vehicular emission and industries. Studies by Lam et al. (1999) reported a high degree of correlation (0.89) between monthly mean $PM_{2.5}$ and NO_2, which indicates that a major source of $PM_{2.5}$ is from automobile exhaust. The annual mean $PM_{2.5}$ mass at different stations ranges from 34.5 ± 17.4 to $60.0 \pm 17.0 \mu g\,m^{-3}$, which is almost 2–4 times larger than USEPA standard annual mean of $15 \mu g\,m^{-3}$. These annual values compare well with reported annual mean for the year 2000–2001 (Louie et al., 2005).

Delhi, the capital of India, is one of the 10 most polluted cities in the world with a human population of 14 million. The estimated emission of pollutants from automobiles in Delhi exceeds 1300 tons every year (Goyal and Sidhartha, 2003) and contributes almost 70% of the total pollution in Delhi. However, depending on local meteorological conditions, high concentration of PM could also come from natural dust, which could be transported to the site or local roadside dust. The overall contribution of dust in $PM_{2.5}$ is less compared to its contribution to PM_{10} mass but during dust storm and summer time when wind speed is sufficient high, dust could contribute as much as 20% to the total

$PM_{2.5}$ mass (Hueglin et al., 2005; Zheng et al., 2005). Delhi also has three major thermal power plants in its vicinity which contribute approximately 13% to the total pollution in Delhi (Goyal and Sidhartha, 2003). Fig. 2(d) presents the data from Delhi during 2003. The $PM_{2.5}$ data over Delhi are limited and only available from 23 July to 03 November 2003 and therefore the results should be interpreted with caution. However MODIS AOT data are analyzed for the entire year. Although the air quality of Delhi has improved in recent years, $PM_{2.5}$ concentration in the city ranges from 36 to $52 \mu g\,m^{-3}$, which is two–three times higher than the concentration in Sydney. Here it is important to note that the population of Sydney is around 4.5 million, which is almost one-third of the population in Delhi. The monthly mean AOT values are high during summer and low in winter. The peak AOT was observed in May with an AOT value of 0.9 and the minimum was reported as 0.38 in the February. The AOT value begins to decline as the summer monsoon approaches Delhi in late July or early August, and the decline in the trend of AOT continues until December as a result of washout by the monsoon rain. The winter months (December–February) in Delhi are dominated by cold, dry air and wind speed as low as $1\,m\,s^{-1}$ with ground level inversion, which is one of the reasons for low values of AOT during winter (Goyal and Sidhartha, 2002).

Overall, the air quality in Sydney remains under the 'good' category throughout the year except during the month of December and January, which is largely due to the major bushfire events in the area (Fig. 2(e)). Low values of AOT are seen in the southern hemisphere winter and high values in summer seasons. Aerosol optical thickness over Sydney shows very clear monthly patterns, maximum (0.47) in January and decreases till June (0.1) and then again increasing up to December. The annual mean $PM_{2.5}$ mass ranges from 11.0 ± 7.0 to $15.0 \pm 5.8 \mu g\,m^{-3}$ over different stations in the area, which is within the US EPA standards. The maximum hourly $PM_{2.5}$ values that range from 50.0 to $76.8 \mu g\,m^{-3}$ were also observed during the January 2002 bushfire event in the area.

We calculated the linear correlation coefficient between hourly $PM_{2.5}$ mass and MODIS AOT to examine this relationship quantitatively. Although there are possible uncertainties on the order of 0–10% in $PM_{2.5}$ measurements due to sampling methods and instrument related issues, and uncertainties in

MODIS AOT retrievals (Remer et al., 2005), it is nevertheless a useful tool to estimate local air quality conditions. For example, earlier studies including the one by Wang and Christopher (2003) over 6 stations in Alabama, USA show that there is a high degree of positive correlation (0.7–0.98) between $PM_{2.5}$ concentration and MODIS-derived AOT. However these studies did not account for aerosol MH or vertical distribution of aerosol, which could improve the relationship between $PM_{2.5}$ and MODIS AOT. The poor correlations reported by Engel-Cox et al., (2004) at locations such as California are possibly due to large uncertainties in MODIS AOT retrieval, large variations in vertical distribution of aerosols, and very small values of the actual AOT (as reported by ground-based sunphotometers). A high degree of correlation at any given location shows that most of the pollution is near the surface. In the present study, the highest linear correlation coefficient (0.85) was found over one station in Delhi, and it was lowest (0.11) at the Richmond station in Sydney due to the very low mean optical thickness. Moderate to high correlation coefficient (0.6) is found over New York City region which again confirms that aerosol optical thickness can be a good indicator of PM air quality. Table 1 shows correlation coefficients and other relevant information.

Fig. 3 shows the scatter plot between 24-h averaged $PM_{2.5}$ and AOT derived from Terra

MODIS and Aqua MODIS, respectively over all five regions of study. Data are homogenized only by region and not by other parameters. The different colors in the plot represent five study regions. These 24 hourly averaged $PM_{2.5}$ concentration measurements are used to define air quality indices at each local station. We derived a simple regression equation between MODIS AOT and $PM_{2.5}$ mass concentration by dividing the 24-h mean $PM_{2.5}$ into 11 bins of $5 \, \mu g \, m^{-3}$ intervals. In this way, we can infer air quality categories from satellite data. Fig. 3 also shows these bins with averaged points in MODIS AOT and $PM_{2.5}$ space as black dots and the solid black line shows the regression line between these two parameters. The height of black box represents the standard deviation in MODIS AOT for a particular $PM_{2.5}$ bin. The correlation between bin-averaged AOT and $PM_{2.5}$ concentration is very high, with a linear correlation coefficient about 0.96 for both Terra and Aqua satellites. The linear regression obtained is: MODIS AOT $(0.55 \, \mu m) = 0.006 \times PM_{2.5} \; (\mu g \, m^{-3}) + 0.149$. Using this regression relation MODIS AOT can be quantified into $PM_{2.5}$ concentration and an estimate of the air quality index can be obtained. The linear correlation coefficient between hourly $PM_{2.5}$ and MODIS AOT over an individual region is 0.6 (New York), 0.14 (Switzerland), 0.40 (Hong Kong), 0.41 (Delhi) and 0.35 (Sydney). The low values of
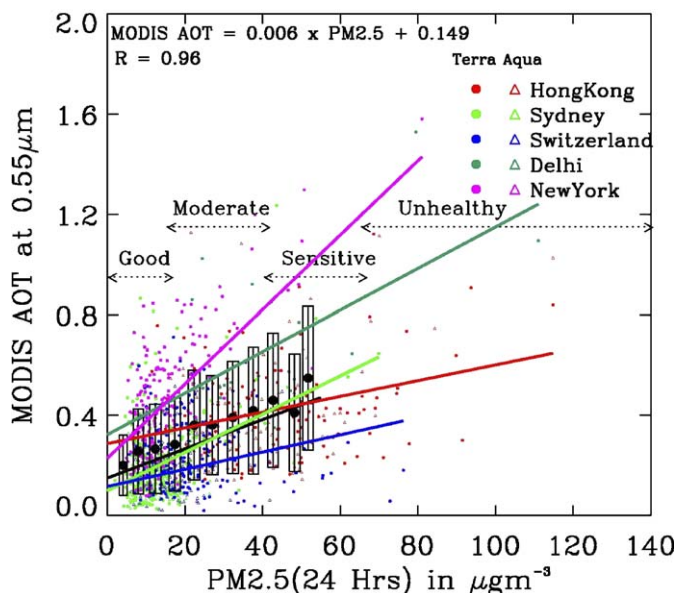

Fig. 3. Relationship between 24-h averaged $PM_{2.5}$ mass concentration ($\mu g \, m^{-3}$) and MODIS aerosol optical depth at $0.55 \, \mu m$. Black rectangular box shows $PM_{2.5}$ bins and dots are averaged values of $PM_{2.5}$ and AOT for those boxes. The horizontal line with two-way arrows in different color shows different air quality limits as described in the text.

correlation coefficients are mainly obtained when MODIS AOT values are small such as over Switzerland and Sydney. The difference in correlation over different study regions indicate the role of other parameters in the $PM_{2.5}$–MODIS AOT relationship, which could vary from region to region. We also note that even when the $PM_{2.5}$ reported values are near zero, the MODIS reports AOT values that are possibly due to the satellite sensing aerosols higher up in the atmosphere when the $PM_{2.5}$ instruments cannot. Although there is strong correlation between hourly $PM_{2.5}$ mass concentration and MODIS AOT, to estimate $PM_{2.5}$ mass concentration from satellite observations several other factors need to be considered such as diurnal variations in $PM_{2.5}$, extinction efficiency, hygroscopic growth factor, RH, and vertical profiles of aerosols (Wang and Christopher, 2003).

4. Sensitivity study

Although MODIS AOT is capable of deriving air quality index (good, moderate, unhealthy) based on derived 24-h $PM_{2.5}$ mass concentration, several meteorological conditions can affect the relationship between AOT and $PM_{2.5}$ mass concentration. The present sensitivity study is designed to quantify the effects of fractional cloud cover (CF), MH, and RH, on the relationship between MODIS-derived AOT and surface measured hourly $PM_{2.5}$ mass concentration.

The effects of RH on AOT are quantified for four different aerosol models (continental clean, continental average, continental polluted, and urban) as described by Hess et al. (1998). In theory, as RH increases the AOT values also increase due to the hygroscopic nature of aerosols (only for hygroscopic particles), which increases the scattering efficiency of the particle. Increases in AOT values are pronounced when RH increases between 90% and 100%. Theoretical calculations show that changing RH values from 98% to 99% can produce more than a 25% change in AOT value (0.6–0.8) whereas there is less than 5% increase in AOT values for change in RH from 50% to 80%.

To estimate the effect of cloud cover on the AOT–$PM_{2.5}$ relationship, data from four stations were analyzed. Data from $PM_{2.5}$ station located in El Paso (CAMS-12) were not considered for this analysis due its high elevation (1169 m above sea level). Table 2 contains details on these datasets.

Linear correlation coefficient (LCC) of 0.69 was obtained between $PM_{2.5}$ and AOT using all 551 data points. Now, to estimate the effects of cloud cover on AOT–$PM_{2.5}$ relationship, all the data points were grouped in four cloud cover ranges as shown in Fig. 4(a). The calculated linear correlations are within 95% significant level. Fig. 4(a) clearly shows that AOT–$PM_{2.5}$ relationship is strongest with LCC equal to 0.78 when cloud cover is less than 25%. The values of LCC decreases as fractional cloud cover increases and reaches to a minimum value of 0.5 when cloud cover is more than 75%. Hence there is an improvement of more than 50% in LCC values when AOT–$PM_{2.5}$ relationship is analyzed under less than 25% cloud cover. Based on our analysis, we conclude that MODIS AOT can be better representative of ground level pollution under cloud free conditions and there could be fewer uncertainties in derived $PM_{2.5}$ mass concentration using regression models based on MODIS AOT. Therefore when conducting studies of MODIS AOT for PM air quality, the data should be screened for cloud cover.

The MH of the atmosphere is a key parameter for the assessment of pollutant distribution from both local and regional sources (Joffre et al., 2001). Aerosols are usually well mixed in the mixing layer of the atmosphere. MHs can be obtained from lidar observations, but dense ground-based lidar network throughout the world is not currently available. Space borne lidars such as the Cloud-Aerosol Lidar and Infrared Pathfinder Satellite Observation (CALIPSO) can provide useful information in the future. Meteorological fields can also be used to provide a first estimate of the MHs of the atmosphere. In general, the MH is calculated by combining mechanical MH (due to winds) and convective MH (due to temperature). In order to estimate the convective MH, vertical profile of temperature is essential. However, it is difficult to get radiosonde observed vertical temperature profiles that coincide with the satellite overpass time and $PM_{2.5}$ station locations. Therefore, the mechanical MH of the atmosphere was estimated using surface wind speed measurements with empirical relationships (Benkley and Schulman, 1979), which provide a good representation of actual MH when compared with SODAR-derived MH (Burzynski et al., 2004). Surface wind speed measurements from $PM_{2.5}$ stations, collocated in space and time with MODIS pixels were used to calculate MH for the entire year over all 5 stations.

Table 2
Statistics of annual average PM$_{2.5}$, MODIS AOT, MODIS cloud cover, relative humidity, and mixing height over 5 stations in Texas. These data are used to perform sensitivity study

Station	Variable	Min	Max	Mean	STD	N
All stations together	MODIS AOT	0.06	1.49	0.35	0.22	901
	PM$_{2.5}$ (μg m^{-3})	1.51	82.32	9.33	8.72	800
	Cloud cover (%)	0.00	94.00	28.74	27.07	860
	Relative humidity (%)	2.90	99.40	43.74	18.70	882
	Mixing height (m)	106.17	1279.65	465.98	201.22	924
CAMS-113 (9.73N and 95.26W)	MODIS AOT	0.06	0.94	0.31	0.20	168
	PM$_{2.5}$ (μg m^{-3})	1.58	50.70	12.14	10.14	157
	Cloud cover (%)	0.00	94.00	35.85	29.89	168
	Relative humidity (%)	30.70	99.40	61.39	16.02	130
	Mixing height (m)	106.17	894.08	384.51	166.19	168
CAMS-12 (1.77N and 106.50W)	MODIS AOT	0.09	1.49	0.52	0.22	218
	PM$_{2.5}$ (μg m^{-3})	1.51	82.32	7.01	7.83	166
	Cloud cover (%)	0.00	74.00	22.42	21.56	218
	Relative humidity (%)	2.90	69.70	22.09	12.09	218
	Mixing height (m)	139.70	1123.19	425.87	156.26	218
CAMS-152 (9.26N and 94.86W)	MODIS AOT	0.06	0.93	0.36	0.19	151
	PM$_{2.5}$ (μg m^{-3})	1.56	50.78	9.27	8.37	141
	Cloud cover (%)	0.00	69.00	19.02	20.29	82
	Relative humidity (%)	27.60	88.90	58.32	12.28	150
	Mixing height (m)	195.58	1279.65	635.13	229.59	150
CAMS-71 (2.56N and 96.32W)	MODIS AOT	0.06	1.12	0.25	0.18	187
	PM$_{2.5}$ (μg m^{-3})	1.52	41.81	8.19	6.89	181
	Cloud cover (%)	0.00	93.00	28.17	27.18	214
	Relative humidity (%)	16.80	67.80	42.99	10.43	214
	Mixing height (m)	173.23	1223.77	493.84	202.13	213
CAMS-8 (9.90N and 95.33W)	MODIS AOT	0.06	0.98	0.28	0.19	177
	PM$_{2.5}$ (μg m^{-3})	1.55	50.37	10.37	9.44	155
	Cloud cover (%)	0.00	92.67	34.92	29.79	178
	Relative humidity (%)	22.40	82.50	46.10	11.45	170
	Mixing height (m)	167.64	938.78	415.27	162.12	175

The data were binned in different range of MH values as shown in Fig. 4(b). Linear correlation coefficients are calculated within 95% significance level. The overall 0.44 LCC between 784 data points is shown as a horizontal dotted line. Maximum LCC values of 0.8 are observed for the first MH bin ranging from 100 to 200 m (29 such data points). This is due to the low MH and since almost all the aerosols were present near surface, the columnar MODIS AOT would agree well with the PM$_{2.5}$ values. In the case of low MH, satellite will observe almost the same amount of aerosol mass as observed by ground instruments. But in the case of larger MH, satellite still observes the same aerosols (as satellites measure columnar loading) and ground instruments observe smaller mass concentrations of aerosols near the ground. Hence in the case of low MH, the MODIS AOT represents the surface measurements well. For 100–200 m MH bin, the LCC value increased to 0.94 (only 16 such measurements exist in data set) when only those measurements taken for which RH of less than 50% were observed. As described earlier, the TEOM measures the PM$_{2.5}$ mass under RH conditions between 40–50%. Hence PM$_{2.5}$ values represent dry aerosol mass, and under dry conditions (RH < 50%) MODIS AOT could be better representative of PM$_{2.5}$ mass concentration. When MHs are close to 1 km (800–1300 m), the bin averaged MH increases as the value of LCC decreases to 0.36. Hence the AOT–PM$_{2.5}$ relationship strongly depends on the height of the mixing layer in the atmosphere. The AOT–PM$_{2.5}$ relationship changes significantly with changes in MH.
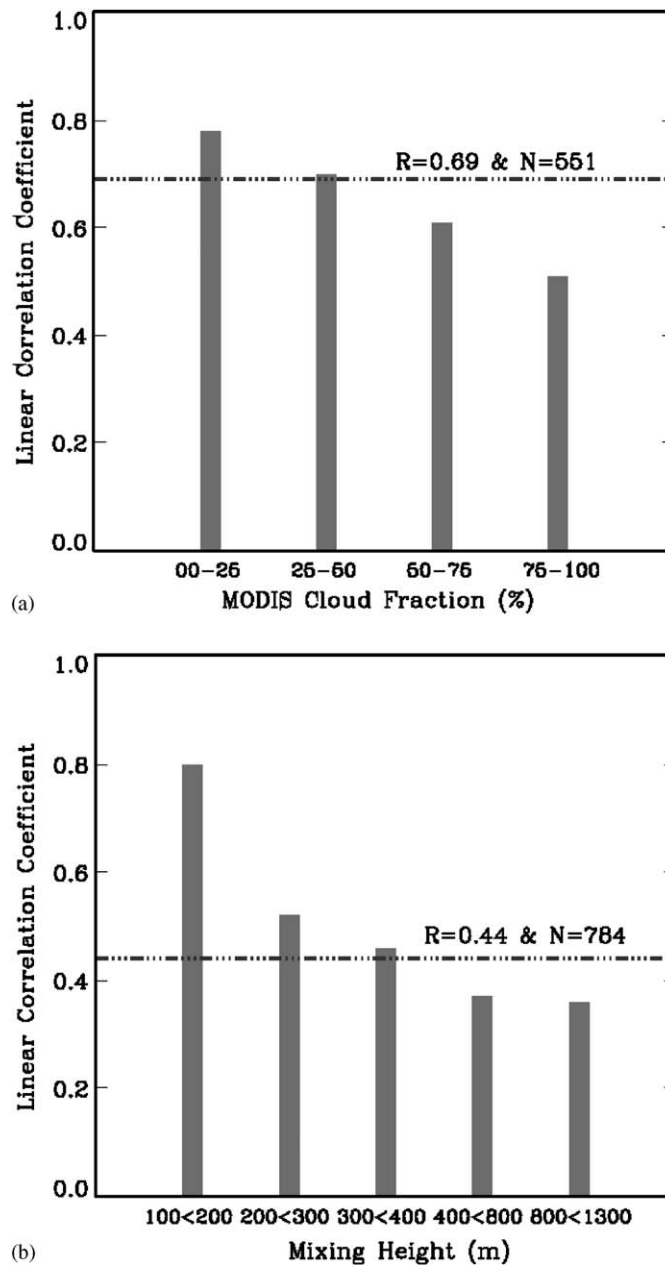
Fig. 4. (a) The effect of MODIS cloud cover (b) effect of atmospheric mixing height on the linear correlation coefficient between PM$_{2.5}$ mass and MODIS AOT.

5. Summary and conclusions

Using MODIS-derived AOT on NASA's Terra and Aqua satellites along with collocated ground-based PM$_{2.5}$ concentration measurements at 26 stations spread over five different geographical regions of the world, we examined PM air quality based on the United States EPA standards. Using regression analysis, we derived empirical relation-

ship between 24 h PM$_{2.5}$ mass concentration ($\mu g\,m^{-3}$) and MODIS AOT (at 0.55 μm) and conclude that the satellite derived AOT is an excellent tool for air quality studies over large spatial area. Our study confirms previous regional and global studies over limited locations (e.g. Chu et al., 2003; Wang and Christopher, 2003). Since PM$_{2.5}$ represents point observations they do not capture the pollution over large areas and satellite

data can now be used in areas where ground measurements are not available. If there is transport of pollutant from one region to another region, then surface measurements cannot capture the synoptic nature of these events and it is difficult to identify the source of pollutants. Since satellite measurements are routinely available on a global basis, the transportation of pollutants can be examined. Along with these datasets, local wind patterns using wind data can be important to identify the sources of pollutants. The satellite–$PM_{2.5}$ correlations are high for cloud free conditions, low boundary level heights, when AOT are higher than about 0.1 and for low RH. However aerosol vertical distribution data are needed along with meteorological data sets to further refine our analysis. Regional analysis shows that air quality condition is good in Sydney and Switzerland whereas it is worst in Hong Kong and Delhi and moderate in New York City during the study period.

Acknowledgments

References

Benkley, W.C., Schulman, L.L., 1979. Estimating hourly mixing depth from historical meteorological data. Journal Applied Meteorology 18.

Burzynski, J., Godlowska, J., Tomaszewska, A. M., Walczewski, J., 2004. The calculated mixing height in comparison with measured data. In: Ninth International Conference on Harmonisation within Atmospheric Dispersion Modelling for Regulatory Purposes.

Hueglin, C., Gehrig, R., Baltensperger, U., Gysel, M., Monn, C., Vonmont, H., 2005. Chemical characterisation of $PM_{2.5}$, PM_{10} and coarse particles at urban, near-city and rural sites in Switzerland. Atmospheric Environment 39, 637–651.

Chu, D.A., Kaufman, Y.J., Zibordi, G., Chern, J.D., Mao, J., Li, C., Holben, B.N., 2003. Global monitoring of air pollution over land from the Earth observing System-Terra Moderate Resolution Imaging Spectroradiometer (MODIS). Journal of Geophysical Research 108, D21.

Draxler, R.R., 2003. Evaluation of an ensemble dispersion calculation. Journal of Applied Meteorology 42, 308–317.

Duce, R.A., Unni, C.K., Ray, B.J., Prospero, J.M., Merrill, J.T., 1980. Long-range atmospheric transport of soil dust from Asia to the tropical North Pacific: temporal variability. Science 209, 1522–1524.

Engel-Cox, J.A., Christopher, H.H., Coutant, B.W., Hoff, R.M., 2004. Qualitative and quantitative evaluation of MODIS satellite sensor data for regional and urban scale air quality. Atmospheric Environment 38, 2495–2509.

Franke, K., Ansmann, A., Müller, D., Althausen, D., Venkataraman, C., Reddy, M.S., Wagner, F., Scheele, R., 2003. Optical properties of the Indo-Asian haze layer over the tropical Indian Ocean. Journal of Geophysical Research 108 (D2), 4059.

Gehrig, R., Buchmann, B., 2003. Characterizing seasonal variations and spatial distribution of ambient PM_{10} and $PM_{2.5}$ concentrations based on long term Swiss monitoring data. Atmospheric Environment 37, 2571–2580.

Goyal, P., Sidhartha, 2002. Effect of winds on SO_2 and SPM concentrations in Delhi. Atmospheric Environment 36 (17), 2925–2930.

Goyal, P., Sidhartha, 2003. Present scenario of air quality in Delhi: a case study of CNG implementation. Atmospheric Environment 37 (38), 5423–5431.

Hazenkamp-von Arx, M.E., Götschi Fellmann, T., Oglesby, L., Ackermann-Liebrich, U., Gislason, T., Heinrich, J., Jarvis, D., Luczynska, C., Jaen Manzanera, A., Modig, L., Norbäck, D., Pfeifer, A., Poli, A., Ponzio, M., Soon, A., Vermeire, P., Künzli, N., 2003. $PM_{2.5}$ assessment in 21 European study centers of ECRHS II: method and first results. Journal of the Air and Waste Management Association 53, 617–628.

Hazenkamp-von Arx, M.E., Götschi, T., Ackermann-Liebrich, U., Bono, R., Burney, P., Cyrys, J., Jarvis, D., Lillienberg, L., Luczynska, C., Maldonado, J.A., et al., 2004. $PM_{2.5}$ and NO_2 assessment in 21 European study centres of ECRHS II: annual means and seasonal differences. Atmospheric Environment 38 (13), 1943–1953.

Hess, M., Koepke, P., Schult, I., 1998. Optical properties of aerosols and clouds: the software package OPAC. Bulletin of the American Meteorological Society 79, 831–844.

Hoff, R.M., Palm, S.P., Engel-Cox, J.A., Spinhime, J., 2005. GLAS long-range transport observation of the 2003 California forest fire plumes to the northeastern US. Geophysical Research Letters 30, L22S08.

Joffre, K.A., Kukkonen, S.M., Bremer, P., 2001. Evaluation of inversion strengths and mixing heights during extremely stable atmospheric stratification. International Journal of Environment and Pollution 16, 1–6.

Kaufman, Y.J., Tanre, D., Boucher, O., 2002. A satellite view of aerosols in climate systems. Nature 419, 215–223.

Kaufman, Y.J., Haywood, J.M., Hobbs, P.V., Hart, W., Kleidman, R., Schmid, B., 2003. Remote sensing of vertical distributions of smoke aerosol off the coast of Africa. Geophysical Research Letters 30 (16), 1831.

Krewski, D., Burnett, R.T., Goldberg, M.S., Hoover, K., Siemiatycki, J., Jerrett, M., Abrahamowicz, A., White,

W.H., 2000. Reanalysis of the Harvard Six Cities Study and the American Cancer Society Study of Particulate Air Pollution and Mortality: A Special Report of the Institute's Particle Epidemiology Reanalysis Project. Health Effects Institute, Cambridge MA, (97pp).

Lam, G.C.K., Leung, D.Y.C., Niewiadomski, M., Pang, S.W., Lee, A.W.F., Louie, P.K.K., 1999. Street-level concentrations of nitrogen dioxide and suspended particulate matter in Hong Kong. Atmospheric Environment 33, 1–11.

Lee, Y.C., Hills, P.R., 2003. Cool season pollution episodes in Hong Kong, 1996–2002. Atmospheric Environment 37, 2927–2939.

Leeuwen, F.X., Rolaf, V., 2002. A European perspective on hazardous air pollutants. Toxicology 181–182, 355–359.

Liu, Y., Park, R.J., Jacob, D.J., Li, Q., Kilaru, V., Sarnat, J.A., 2004. Mapping annual mean ground-level $PM_{2.5}$ concentrations using Multiangle Imaging Spectroradiometer aerosol optical thickness over the contiguous United States. Journal of Geophysical Research 109, D22206.

Louie, P.K.K., Watson, J.G., Chow, J.C., Chen, A., Sin, D.W.M., Lau, A.K.H., 2005. Seasonal characteristics and regional transport of $PM_{2.5}$ in Hong Kong. Atmospheric Environment 39 (9), 1695–1710.

Pope, C.A., 2000. Epidemiology of Fine Particulate Air Pollution and Human Health: Biologic Mechanisms and Who's at Risk? Environment Health Perspective 104 (Supl. 4), 713–723.

Remer, L.A., Kaufman, Y.J., Tanré, D., Mattoo, S., Chu, D.A., Martins, J.V., Li, R-R., Ichoku, C., Levy, R.C., Kleidman, R.G., Eck, T.F., Vermote, E., Holben, B.N., 2005. The MODIS Aerosol Algorithm, Products and Validation. Journal of the Atmospheric Sciences 62, 947–973.

Schwab, J.J., Felton, H.D., Demerjian, K.L., 2004. Aerosol chemical composition in New York state from integrated filter samples: urban/rural and seasonal contrasts. Journal of Geophysical Research 109, D16S05.

Slater, J.F., Dibb, J.E., 2004. Relationships between surface and column aerosol radiative properties and air mass transport at a rural New England site. Journal of Geophysical Research 109, D01303.

TERI, 2001. Review of past and on-going work on urban air quality in India. Report submitted to the World Bank, December, Tata Energy Research Institute, 2001EE41.

United States Environmental Protection Agency (USEPA), 2003. Air Quality Index, A Guide to Air Quality and Your Health. EPA-454/K-03-002.

Wang, J., Christopher, S.A., 2003. Intercomparison between satellite-derived aerosol optical thickness and $PM_{2.5}$ mass: implications for air quality studies. Geophysical Research Letters 30 (21), 2095.

World Urbanization Prospects: The 2003 revision. United Nations Department of Economic and Social Affairs, Population Division, New York.

Zhang, J., Reid, J.S., Holben, B.N., 2005. An analysis of potential cloud artifacts in MODIS over ocean aerosol optical thickness products. Geophysical Research Letters 32, L15803.

Zheng, M., Salmon, L.G., Schauer, J.J., Zeng, L., Kiang, C.S., Zhang, Y., Cass, G.R., 2005. Seasonal trends in $PM_{2.5}$ contributions in Beijing China. Atmospheric Environment 39, 3967–3976.